NUMERICAL OPTIMIZATION: AN ASSESSMENT OF ITS ROLE IN TRANSPORT AIRCRAFT AERODYNAMIC DESIGN THROUGH A CASE STUDY*

Manuel E. Lores and Peter R. Smith
Lockheed-Georgia Company
Marietta, Georgia

and

Robert A. Large, Captain, USAF
Flight Dynamics Laboratory
Wright-Patterson AFB, Ohio

Abstract

An efficient transonic wing design procedure based upon numerical optimization together with three-dimensional transonic methods has been developed and used to design an advanced transport wing. The method development included an examination of the use of both full potential and extended small disturbance analysis codes and demonstrated that the former formulation was more reliable. In either case, the design procedure is economical and easy to use. Design verification in a unique semi-span test arrangement demonstrated that the design method produced a wing which satisfied the study design requirements. However, aeroelastic deformation of the wing occurred during the wind tunnel test. The computational methods used in the design procedure were employed to assess the effect of the aeroelastic deformation. The paper concludes with an evaluation of the design procedure and recommendation for its improvement.

Introduction

Efficient transonic performance continues to be an important aircraft design requirement. For transport category aircraft, improved cruise efficiency as manifested by reduced fuel consumption is demanded by escalating fuel costs. Accurate computational design methods are required to develop the sophisticated aerodynamic configurations needed to produce the desired aerodynamic efficiency. The methods are also required because the increasing costs of wind tunnel tests together with the interference and scale problems associated with tests conducted at transonic conditions[1,2] make total reliance on experimental configuration development impractical.

Recent improvements in computational aerodynamics have permitted rapid, efficient, and relatively accurate solution of the nonlinear partial differential equations which describe the transonic flow about aircraft. These improvements have resulted in the availability of numerous 3-D transonic flow analysis methods[3,4,5,6]. Analysis methods have provided the ability not only to better understand the physics of transonic flows, but also to design efficient transonic configurations. However, design by repeated application of analysis codes is wasteful of both computer and manpower resources, and provides no assurances that an optimized design will result. In addition, considerable user expertise is required to forecast the effects of geometric perturbations on aircraft aerodynamics.

There is, therefore, a need for a 3-D transonic computational design procedure. To be complete, the procedure must not only include efficient and reliable computational design methods, but also must provide a means for effectively incorporating the methods in the aircraft aerodynamic design process.

Numerical optimization has recently received considerable attention as an aerodynamic design method. In this design approach, a numerical minimization scheme is coupled with an aerodynamic analysis method to design geometries that are in some sense optimized for specific flight conditions. The capability is thus offered of using proven analysis codes in a systematic design process rather than developing new inverse transonic design methods. References 7, 8, and 9 describe recent applications of numerical optimization in transonic three-dimensional wing design.

This paper describes the use of numerical optimization with modern three-dimensional transonic codes in the cruise aerodynamic design of a transport wing. First, the mission and the airplane configuration is reviewed, and the design objective is defined. This discussion is followed by a detailed description of the wing numerical design method and its application. The associated wind tunnel test is then described, and aircraft performance with the new wing is compared to that of the baseline configuration. Next, computed aerodynamics are compared with measured data. Finally, the entire design procedure is reviewed and recommendations are made for its improvement.

Mission and Configuration

At the start of the design study, the political and economic environment relative to military transport aircraft made the development of a derivative aircraft a more realistic prospect than the development of a completely new transport aircraft for which design requirements were not clearly defined. The derivative must, of course, exhibit significantly improved performance for the original mission, or increased ability to perform alternate missions.

* *This work was supported by the United States Air Force and the Ames Research Center, NASA, under USAF Contract No. F33615-78-C-3014.*

Mission Definition and Design Goal

Operation of the USAF C-141 fleet accounts for approximately 15% of the total Air Force fuel allotment. Since this aircraft plays an important role in USAF logistics and uses a significant amount of fuel, aircraft modifications to improve its efficiency are of interest. Furthermore, because the general arrangement and mission of the C-141 are representative of current and planned military transports, aerodynamic technologies developed using the C-141 as a case study can be expected to be of general applicability.

A twin-engined active control derivative of the C-141B was selected as the case study aircraft. The derivative is designated herein as the C-141B/AC2; it is designed to carry a 75,000 pound payload 3,500 nautical miles at 0.80 Mach number. The cruise Mach number of 0.80 was selected instead of the 0.77 cruise Mach number of the C-141B to improve productivity and to provide a more challenging transonic design problem. Performance constraints include a field length of 7,500 feet and an initial cruise altitude of 35,000 feet. The predicted range and payload of the derivative aircraft are compared to those of the C-141B in Figure 1.

The design goal of this study was to significantly reduce the C-141B/AC2 empty weight (OWE) and fuel requirements from those of the C-141B.

Aircraft	Empty Weight
C-141B	148526 LB
C-141B/AC2	118300 LB

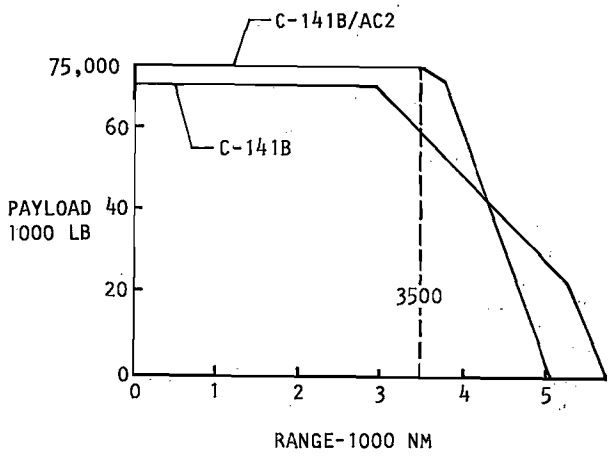

Figure 1. Predicted Performance

Configuration Development

The C-141B/AC2 configuration was sized using the Lockheed-Georgia General Aircraft Sizing Program (GASP), a proprietary computer program presently used for all company preliminary design studies. The program accounts for the interaction of the various design constraints and technical disciplines involved in the aircraft design process. Technology levels for the various disciplines are controlled by the use of input adjusting factors. The C-141B/AC2 aircraft has been sized using advanced technology levels which are appropriate to an initial operational capability date in the mid-1980s.

A matrix of configuration variables was examined to determine the minimum fuel aircraft which met the design mission. The range of variables considered was:

Wing Loading	100 to 140 LB/FT^2
Aspect Ratio	8 to 12
Wing Sweep	10 to 25 DEG
Initial Cruise Altitude	31,000 to 35,000 FT
Cruise Power Setting	0.7 to 1.0

The constraints imposed on the parametric designs were:

Fuel Volume Ratio (Fuel Volume Available/Fuel Required for 3500 NM)	$\geq$ 1.0
Field Length	$\leq$ 7,500 FT
Aspect Ratio	$\leq$ 12
Cruise Altitude	$\geq$ 31,000 FT

Configuration Characteristics and Performance

The general arrangement of the C-141B/AC2 is shown in Figure 2. Based on the technology levels used in the aircraft sizing, the C-141B/AC2 predicted OWE is approximately 75% of the C-141B, and the former aircraft requires approximately 44% of the fuel used by the latter airplane. These improvements are obtained using an aspect ratio 12 wing with a quarter chord sweep of 25^o and an average thickness to chord ratio of .109. As will be shown, the use of the new design procedure produced a significantly thicker wing with only minor performance degradations.

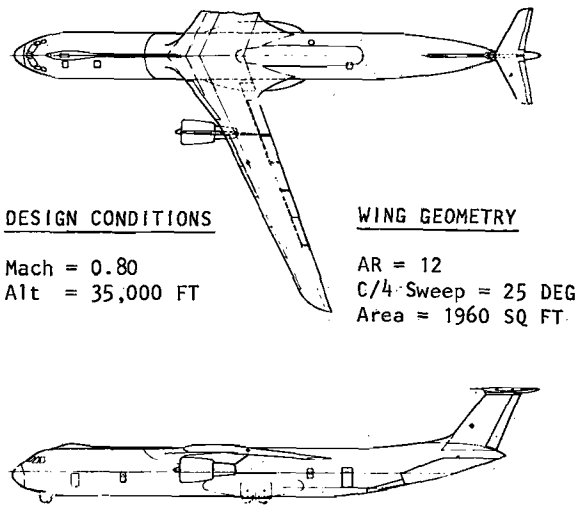

Figure 2. C-141B/AC2 General Configuration

Impact of Advanced Technologies

The C-141B/AC2 performance discussed above is made possible by the incorporation of the following advanced technologies:

- o High Aspect Ratio, Supercritical Wing
- o Advanced Engines
- o Composite Materials
- o Active Controls

Active controls are used for load alleviation, stability augmentation, flutter suppression, and ride enhancement. The performance improvement as reflected in reduced fuel and gross weight brought about by each of the technologies is shown in Figure 3. Clearly, the major performance improvements result from the use of modern engines and advanced technology high aspect ratio wing. The C-141B/AC2 wing cruise aerodynamic design forms the basis for the validation of the transport design procedure.

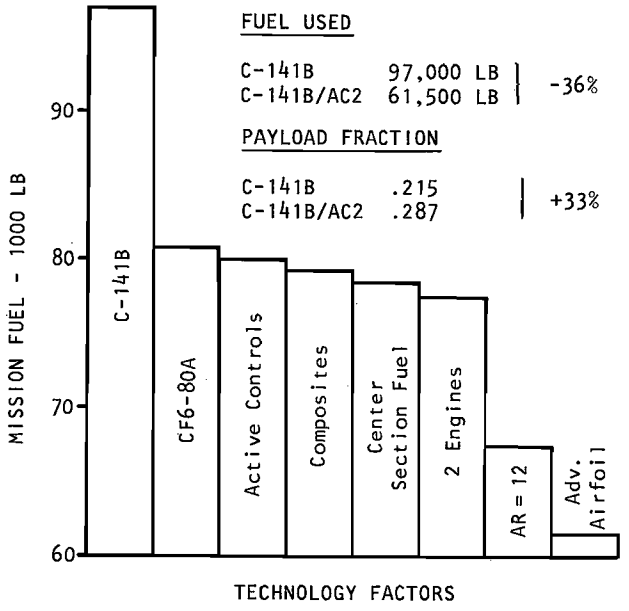

Figure 3. Technology Benefits

Design Procedure

The transport wing design procedure is shown schematically in Figure 4. The procedure is based upon the use of an isolated wing code for the transonic design, and the use of a more economical subsonic panel method which provides good geometric resolution to compute interference pressures. (Example: On lower wing surface due to gear pod.) Also included in the design procedure is a systematic approach for selecting the starting wing geometry.

The key element in the procedure is the use of numerical optimization in the wing design. The wing design code was developed by linking Vanderplaats' constrained function minimization program[10] with three-dimensional isolated wing analysis codes. Both an extended small disturbance code based on a program written by Bailey, Ballhaus, and Frick[3], and Jameson's FL022 full potential equation program[4]

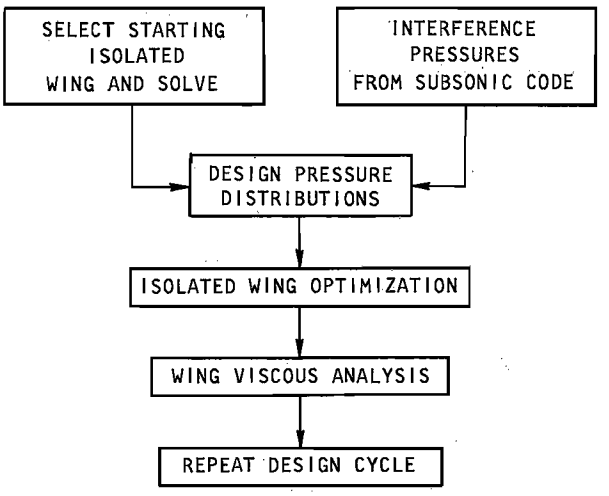

Figure 4. Design Procedure

were used in this study. The design objectives and constraints, and the permissible geometric perturbations (i.e., design variables) are detailed in the following paragraphs.

Design Objective and Constraints

To avoid the use of inaccurately calculated quantities such as drag in the optimization procedure, the design method was developed to permit the design of wings with specified chordwise pressure distributions. The capability of examining two pressure design objectives was provided. One design objective was the minimization of the RMS deviation between the target and actual pressures:

$$OBJ_1 = \left[\sum_N (C_p - C_{p_D})^2 / N \right]^{1/2}$$

where N is the number of pressure coefficients, and C_{PD} is the target pressure coefficient. The second objective considered was

$$OBJ = \sum_N (C_p - C_{p_D}); \text{ Constraint} = C_p < C_{p_D}.$$

Notice the constraint is required to make the second objective meaningful.

Both objectives were tried in the design study, and the first objective proved to be superior. Consequently, OBJ_1 was used in the wing design.

Design Variables

Consistent with established wing geometry definition procedures, the wing geometry is determined by specifying the airfoil sections at various geometric control span stations and connecting these sections by linear loft elements. At each control station, the permissible surface perturbations are listed in Table 1. The magnitude of each of these 14 surface perturbation functions plus the section twist angle are the fifteen design variables available for each surface at each geometric control span station. Thus, for a four control station wing, if all the surface perturbations were used, and if all the sections were designed

simultaneously, a total of 15 variables per surface per station x 2 surfaces x 4 stations = 120 design variables, would be required.

Implementation

The simultaneous use of 120 design variables would result in an inordinately long computer run (greater than 10 hours on a CDC 7600). Job turnaround time on such a run would be very long, and an error would have a catastrophic effect on computer budget. Consequently, wing design was accomplished in a series of steps. First, the upper surface was designed one section at a time proceeding from the root to tip. Next, the lower surface is similarly designed.

The optimization is done using the desired viscous pressure distribution. Consequently, the design procedure produces the "fluid" wing geometry (that is, the desired solid wing geometry plus the boundary layer displacement thickness). The fluid wing is then analyzed and the entire process, or parts thereof, are repeated as required to produce the desired pressures.

Extraction of Solid Wing Geometry

The wing contours produced by the optimization include the boundary layer displacement thickness, δ^*. The solid wing geometry is found by subtracting δ^* from the computed wing contours at each of the design stations. A conventional 2-D integral boundary layer code[11] is used to compute δ^*.

TABLE 1 TRANSPORT WING DESIGN VARIABLES

$V(1) = 3.89\,(X/C)^{.25}\,(1 - X/C)e^{-20\,(X/C)}$

$V(2) = 10.68\,(X/C)^{.5}\,(1 - X/C)e^{-20\,(X/C)}$

$V(j) = \sin^3\,(\pi\,(X/C)^{r_j}),\quad j = 3, 12$

$V(13) = (X/C)^8$

$V(14) = (X/C)^{20}\,e^{a}\,\sqrt{1 - (X/C)}$

$a = .5/(1 - (X/C)_M) - 20\,(X/C)_M$

$(X/C)_M$ = (X/C) for max camber

$V(15) = \theta$ TWIST

Sine deformations

j	r_j	$(X/C)_{Max\ def}$
3	.231	.05
4	.301	.10
5	.431	.20
6	.576	.30
7	.756	.40
8	1.000	.50
9	1.357	.60
10	1.943	.70
11	3.106	.80
12	6.579	.90

Analysis of Optimized Wing

The performance of the optimized wing is investigated using both full potential and extended small disturbance viscous transonic codes. The solid wing geometry is used in these calculations.

Configuration Design

The design procedure was used to design a new wing for the C-141B/AC2 configuration. The goal of this study was to improve the wing aerodynamics and at the same time increase the wing thickness for the Mach = .80, C_L = .60 design condition. Increased wing thickness was sought to increase the fuel volume, and to reduce wing weight.

Current aft-loaded supercritical airfoil technology was used to determine the predicted C-141B/AC2 average wing thickness of 10.9%. Clearly, improvements in wing aerodynamic performance through the use of the new design procedure will be required to design a wing with increased thickness which operated efficiently at Mach = .80 and C_L = .60. The new design method will be shown to be a successful approach for obtaining the desired improvements in aerodynamic efficiency.

Starting Wing Selection

Two starting wings were considered. One wing used airfoil sections developed at NASA-Langley as part of the Energy Efficient Transport Program[12]. The second wing used airfoils designed at Lockheed-Georgia in support of in-house configuration design studies[13]. The wings were analyzed using the extended small disturbance code of Ref. 3. The results of these calculations, which are summarized in Figure 5, show that both wings have well-behaved design point pressures. Thus, either wing is satisfactory for starting the design process.

The wing with the Lockheed airfoils was selected as the starting wing because the airfoils were systematically developed using state-of-the-art airfoil inverse and analysis transonic methods. Consequently, this initial wing design lends itself well for inclusion in a formal design procedure.

Interference Pressures

The use of an isolated wing code during numerical optimization is a key feature of the design method because its use minimizes computer resource

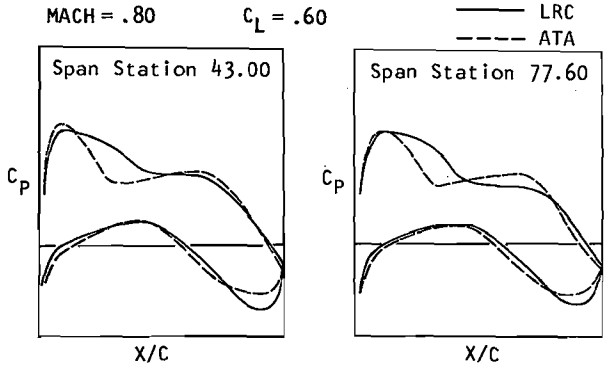

Figure 5. Starting Wing Pressures

requirements while yielding good predictions of upper surface pressures for high-wing configurations. The interference pressure perturbations are confined to the lower surface and are primarily due to the gear pod. Since the flow is subcritical on the lower surface, and since the interference pressures are small, they can be calculated using a subsonic panel method[15] which provides very good geometric resolution in the wing-body-gear pod area as shown in Figure 6.

The calculated isolated wing and wing-body-gear pod pressures are compared in Figure 7 where the lower surface interference pressures are apparent. Incremental interference pressures are computed by subtracting the isolated wing pressures from the complete configuration pressures and multiplying the difference by the ratio of the Prandtl-Glauert factors corresponding to the subsonic analysis and the design Mach numbers. The resulting incremental interference pressures are subtracted from the configuration transonic design pressures to produce the target lower surface pressure distributions.

Design Pressures

Target wing pressures were initially specified near the wing root, break and tip. Subsequently, an additional design station located approximately midway between the break and the tip was found to be necessary. The upper surface pressures were selected to provide a weak shock wave on the outer panel near the 60% chord station. The root pressures were selected to minimize isobar unsweeping and to avoid large trailing edge pressure gradients which might result in the formation of a strong trailing edge shock wave.

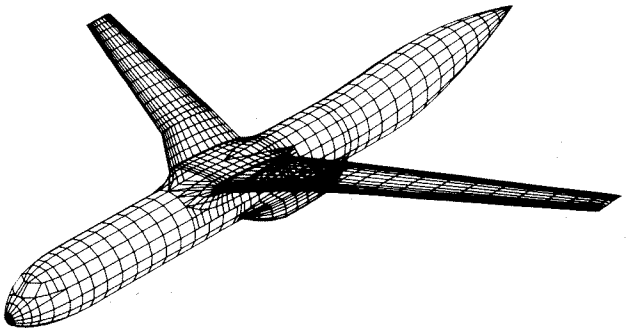

Figure 6. Subsonic Code Modeling

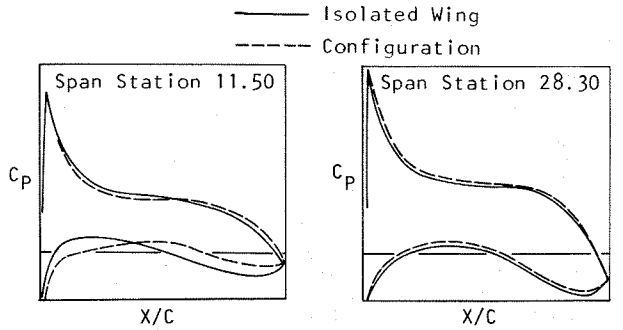

Figure 7. Interference Pressures
Mach = .70 Alpha = .50 Deg

Numerical Optimization

The numerical optimization procedure was used to determine the wing geometry which produces the desired wing pressures. The wing geometry was determined by designing the four wing control stations shown in Figure 8 and using linear lofting to generate intermediate ordinates. Early numerical experiments showed that the 60% span design station was needed because perturbations of the wing tip section were inadequate to control mid-semispan and tip pressures simultaneously. A constant normalized section wing carry-through was used.

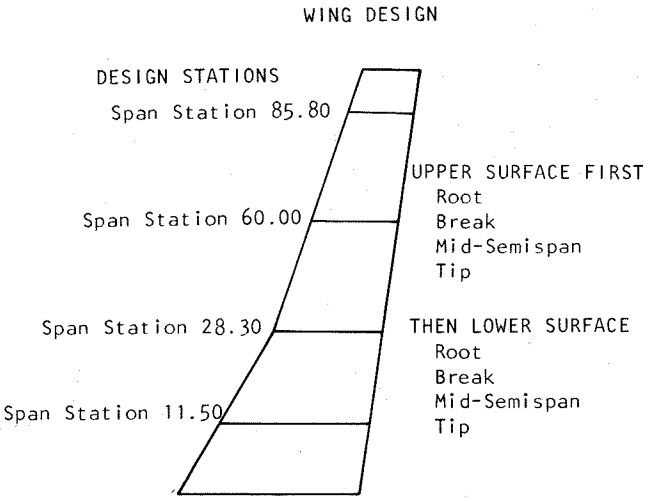

Figure 8. Wing Representation For Design

Of note also in Figure 8 is the specification of tip pressures near the 85% span station. This choice was made because of the relative inaccuracy of computed results near the wing tip.

Extended Small Disturbance Design

The Lockheed extended small disturbance program was used in the initial wing design. The final wing pressures are compared with the target pressures in Figure 9. Also shown here is the agreement between target and computed pressures after the upper surface design of each span station. The agreement between target and computed pressures is fair.

Before continuing with the design process, the solid wing geometry was analyzed using viscous versions of both full potential[4] and extended small disturbance[3] codes. The results of these calculations are shown in Figure 10. On the premise that the FPE results are correct, these data show that the ESD code mispredicts the wing leading edge flow field, and this error causes complete disagreement between ESD and FPE results.

Full Potential Design

The failure of the ESD optimization to design accurately the wing leading edge made a second pass

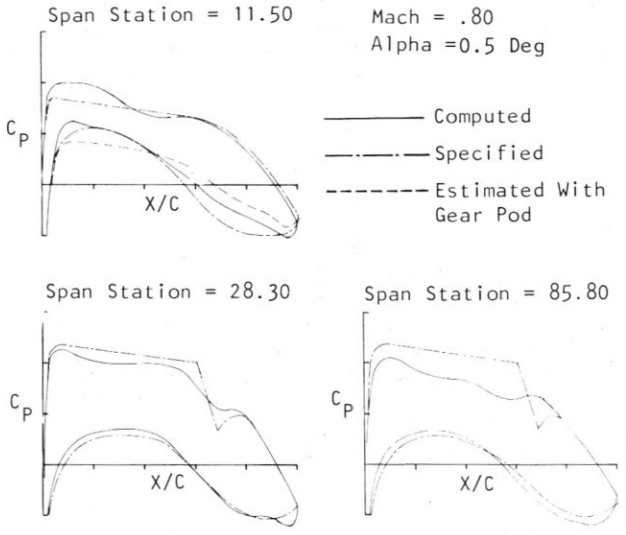

Figure 9. ESD Optimization Pressures

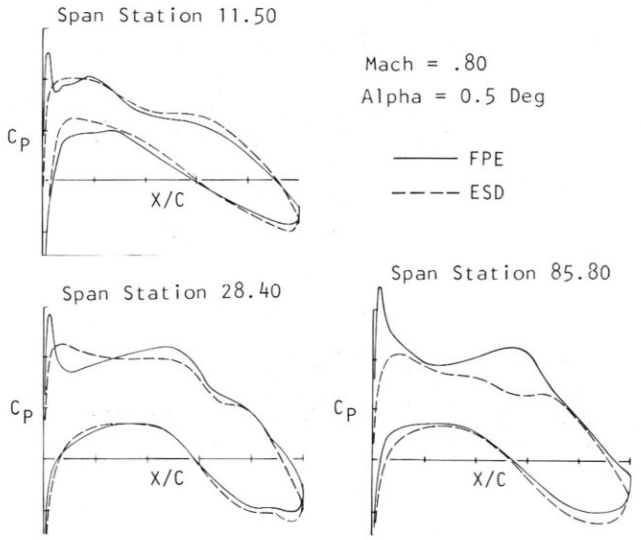

Figure 10. Analysis of ESD Wing

through the design procedure using a full potential equation analysis code necessary. The FPE optimization was done using the design variables and objective used in the ESD optimization. The target pressures were modified to produce a slightly weaker shock wave.

The span load distribution of the resulting wing was not satisfactory because the outboard section of the wing was too highly loaded, while the root section was unloaded. The lower surface of the root was modified using a simple Lockheed linear design method to increase the section loading at a small sacrifice in wing root thickness. The wing twist was also adjusted using a very efficient panel method to decrease the tip loading.

The resulting wing was analyzed using both the FPE and ESD viscous codes. The results are summarized in Figure 11. The codes produce results

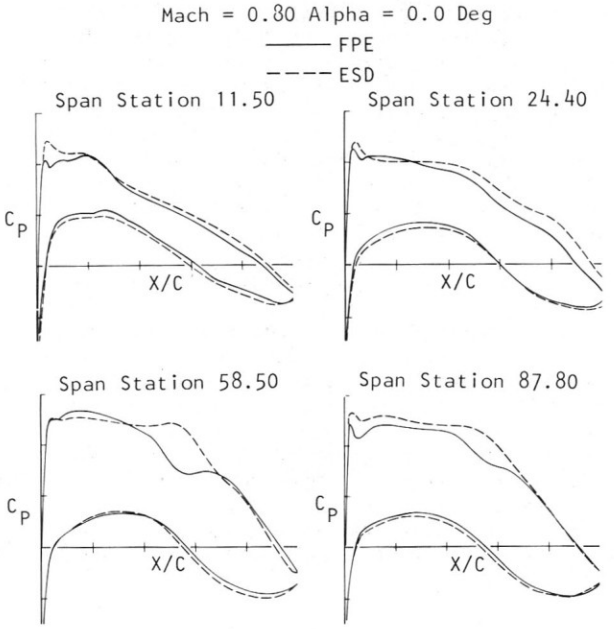

Figure 11. Analysis of FPE Way

in good agreement with one another, indicating that ESD methods yield accurate results if the leading edge is properly designed. The wing pressures are quite satisfactory. There is no tendency for isobars to coalesce near the root trailing edge, nor is there a tendency for a leading edge shock wave to form. The desired mid-chord shock is weak (normal Mach number less than 1.16). Consequently, this FPE-designed wing was selected as the final C-141B/AC2 wing design.

Wind Tunnel Test

Test Facility

The design verification wind tunnel tests were conducted in the Lockheed-Georgia Compressible Flow Wind Tunnel (CFWT). The general arrangement of the CFWT is shown in Figure 12. The tunnel is of the blow-down type, exhausting directly to the atmosphere. The tunnel is capable of producing flows with unit Reynolds numbers up to approximately 55 x 10^6 per foot at M = 0.8. The test section is 50.8 cm (20.0 in.) wide by 71.2 cm (28.0 in.) high by 183 cm (72.0 in.) long and is enclosed in a 3.7 m (12.0 ft.) diameter plenum

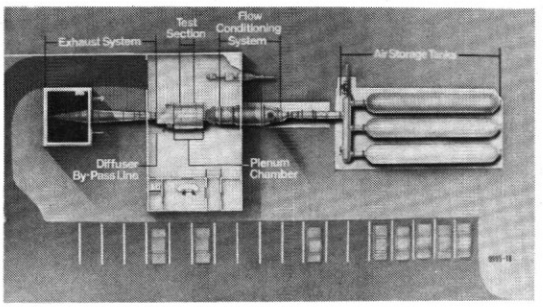

Figure 12. Lockheed-Georgia Compressible Flow Wind Tunnel

chamber. The top and side walls of the three-dimensional test section have variable porosity capability (from 0 to 10 percent). The bottom wall, where the model is mounted, is not porous.

The semi-span configuration of the CFWT is shown in Figure 13. The model is mounted on a five-component balance located in the floor. The balance and model rotate together on a turntable to vary angle of attack. A bleed duct is located 53.6 cm (21 in.) ahead of the balance centerline to remove the wind tunnel boundary layer. The boundary layer bleed system has an independent control valve and exhausts to atmosphere through a separate pipe system. A more detailed description of the facility may be found in Reference 16.

Six far-field pressure rails containing 31 static pressure taps were mounted on the tunnel walls as shown in Figure 13 to provide boundary conditions for code correlations. The far-field measurements were extended to the model centerline by a row of fourteen pressure taps located along the tunnel floor on each side of the model.

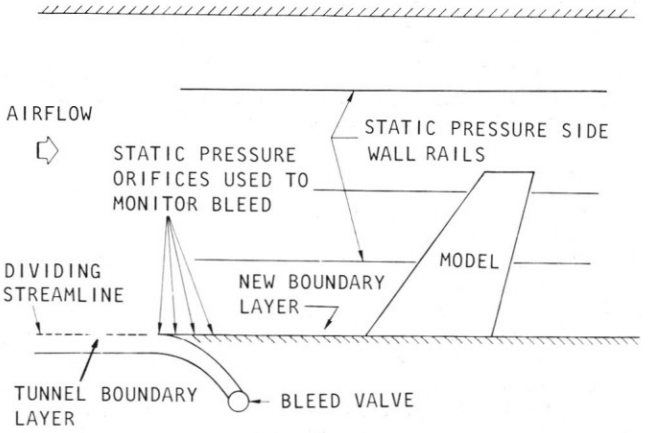

Figure 13. Semi-Span Test Arrangement

Models

An existing .0188 scale C-141 semi-span model, Figure 14, was used to obtain baseline data. The wing on this model is instrumented with 126 surface static pressure taps located at three span stations. The new C-141B/AC2 wing, shown in Figure 15, was machined from a solid billet of 17 stainless steel, and was hand-finished to a tolerance of $\pm$ .05 mm (.002 in.). The wing has a total of 140 static pressure orifices located in chord-wise rows at 5 spanwise stations. The upper surface pressure orifices were installed by drilling completely through the wing so that all tube routing is on the wing lower surface. This installation technique makes the upper surface completely free of tube routing channels which can cause possible discontinuities in curvature that may affect the supersonic flow on the upper surface.

Tests

The tests were conducted at a Reynolds number of 5 million over a Mach number range of 0.60 to 0.84, and an angle of attack range of -2 degrees to +4 degrees. The baseline C-141 model was tested in the semi-span wing configuration with fuselage and gear pod fairing. More extensive configurations including pylons and nacelles were tested for the C-141B/AC2 design.

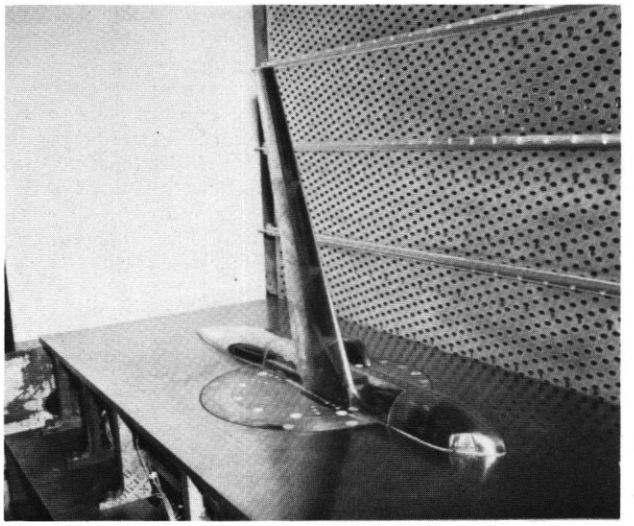

Figure 14. C-141B Model Installation

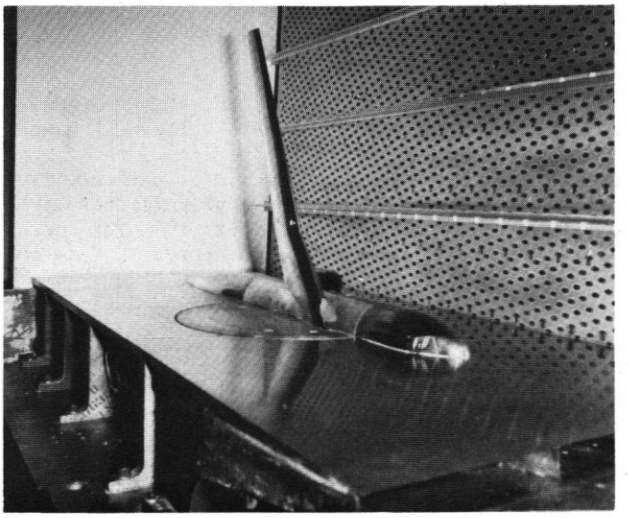

Figure 15. C-141B/AC2 Model Installation

Design Evaluation

Analysis of Test Data

The C-141B/AC2 design conditions and wing geometry are substantially different from the C-141. Consequently, a comparison of wing aerodynamics does not by itself provide a true measure of the effectiveness of the new wing. For example, a comparison of drag polars at the C-141B/AC2 design Mach number would not be meaningful because the C-141 was designed to cruise at .77 Mach, and its wing is well into drag rise at .80 Mach. Consequently, the efficiency of the design procedure is evaluated by comparison of complete airplane performance capabilities rather than by reference to incremental aerodynamic characteristics. To make these comparisons, flight aerodynamics for the C-141B/AC2 are extrapolated from wind tunnel data using the known C-141 flight characteristics as a calibration.

In the Compressible Flow Wind Tunnel, the tunnel top and bottom walls are relatively close - approximately 3½ mean chords - to the wing. Although a procedure for taking wall effects into account is under development[17], time constraints precluded its use in this preliminary evaluation. Accordingly, the analysis method adopted herein is based on a comparison of uncorrected measured and estimated drag differences for the two wing-fuselage-gear pod configurations. The drag estimation technique is known to agree well with C-141 flight experience.

A drag estimation at M = 0.70 was made for each configuration at the wind tunnel Reynolds number and then compared with the measured model drag. The resulting drag differences are shown in Figure 16. The variation with lift coefficient is identical for the two designs, and the C-141B/AC2 drag is 10 counts less than the C-141B drag. The actual drag of the C-141B full-scale aircraft is known from flight tests and is reproduced by the drag estimation method employed. Assuming that the drag increment is insensitive to Reynolds numbers, the full-scale drag of the C-141B/AC2 aircraft at M = 0.70 can be obtained by subtracting 10 counts from the full-scale estimation drag polar for the C-141B.

The next step in the drag analysis procedure was the determination of the drag rise Mach number and the compressibility drag increment. A direct comparison of the measured drag rise characteristics of the wing-fuselage-gear pod configurations at constant C_L is presented in Figure 17. The corresponding drag divergence Mach numbers, M_D, are shown as a function of lift coefficient in Figure 18. The target M_D value for the C-141B/AC2 design of

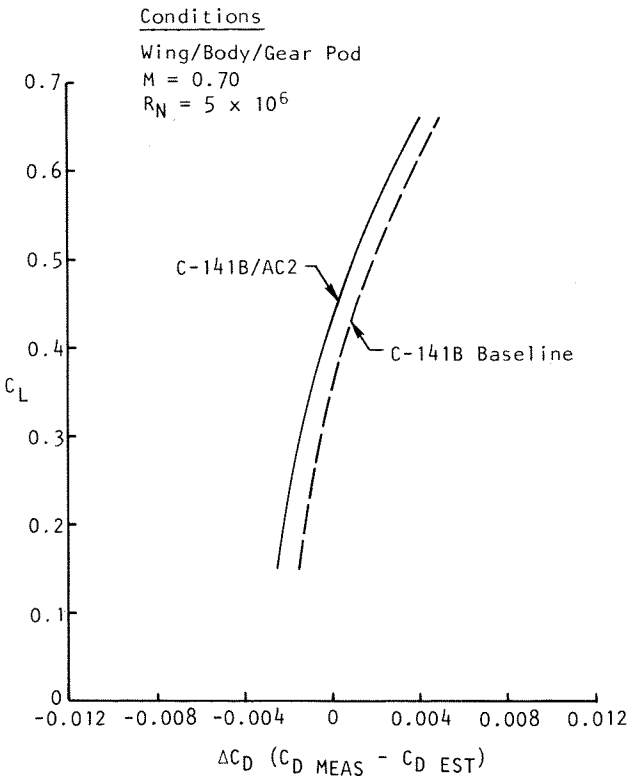

Figure 16. Comparison of Measured Model Drag with Estimates

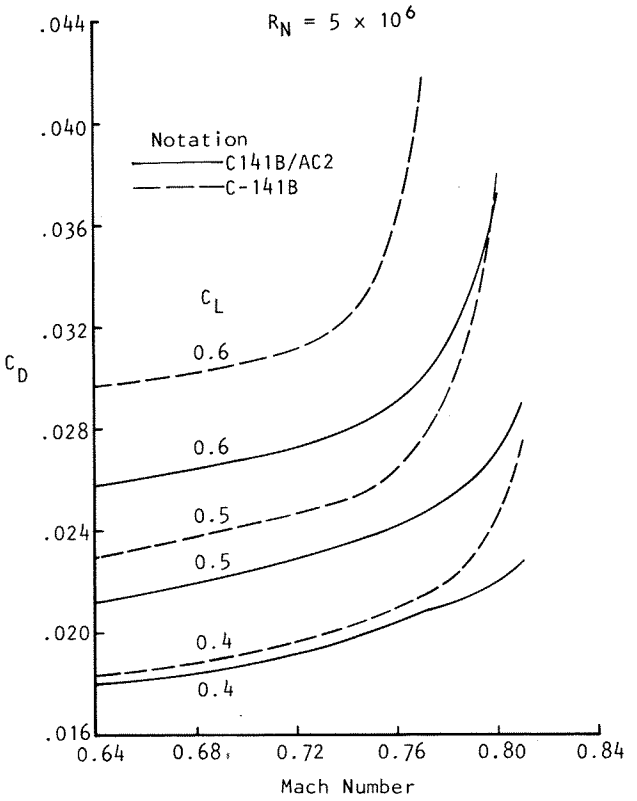

Figure 17. Measured Drag Rise Characteristics

M = 0.80 at C_L = 0.60 was not achieved. This results partly from the viscous uncambering of the cove region at the relatively low tunnel Reynolds number, and partly from the aeroelastic deformation of the model wing at the high dynamic pressures of the Compressible Flow Wind Tunnel. Reducing the full-scale design Mach number and lift coefficient to M = 0.78 and C_L = 0.56 in accordance with the measured data of Figure 18 nevertheless results in a highly satisfactory advanced technology C-141B/AC2 aircraft design.

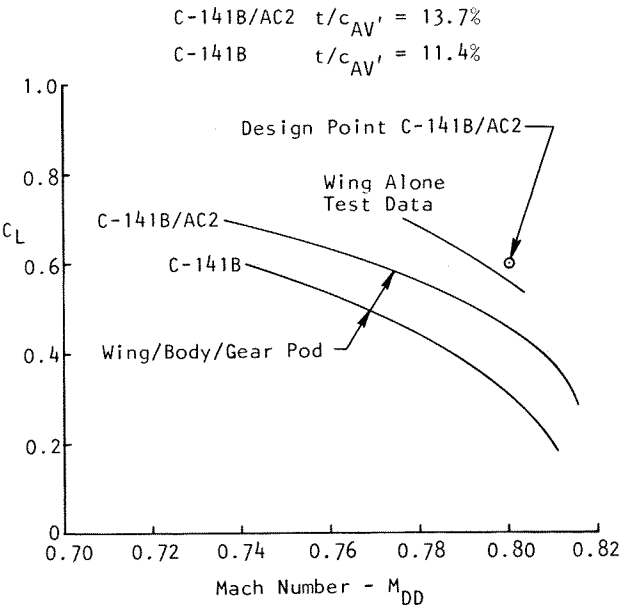

Figure 18. Measured Drag Divergence Mach Numbers

Aircraft Performance

The payload-range performance of the C-141B/AC2 is compared to that of the C-141B and to the C-141B/AC2 target performance in Figure 19. Of note is the better than targeted ferry range of the C-141B/AC2 made possible by the thick wing resulting from the application of the new wing design method. The reduction in aircraft weights and fuel made possible by advanced technology are shown in Figure 20. The predicted gross weight reduction is 2% less than the target value, while the block fuel decrease is 3% greater than targeted. The target empty weight reduction of 20% was achieved. Thus, with the exception of the .80 cruise Mach number, the study design objectives have been achieved.

Preliminary Correlations

The experimental program was planned to provide an extensive data set particularly well-suited for code correlations. Specifically, pressure and force data are available for the following C-141B/AC2 configurations:

- o Isolated Wing
- o Wing + Pylon/Nacelle
- o Wing + Fuselage
- o Wing + Fuselage + Pylon/Nacelle
- o Wing + Fuselage + Gear Pod
- o Wing + Fuselage + Pylon/Nacelle + Gear Pod

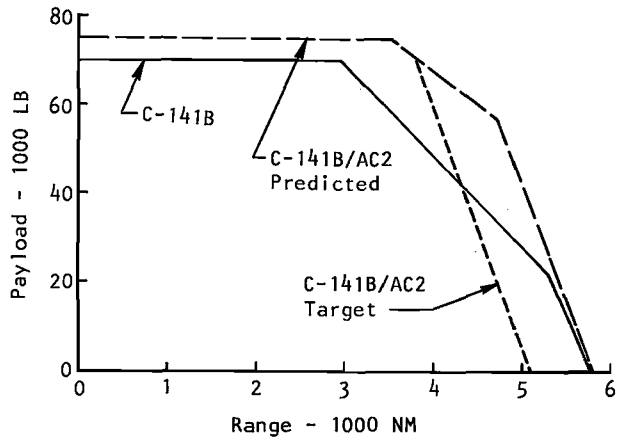

Figure 19. Payload - Range Performance

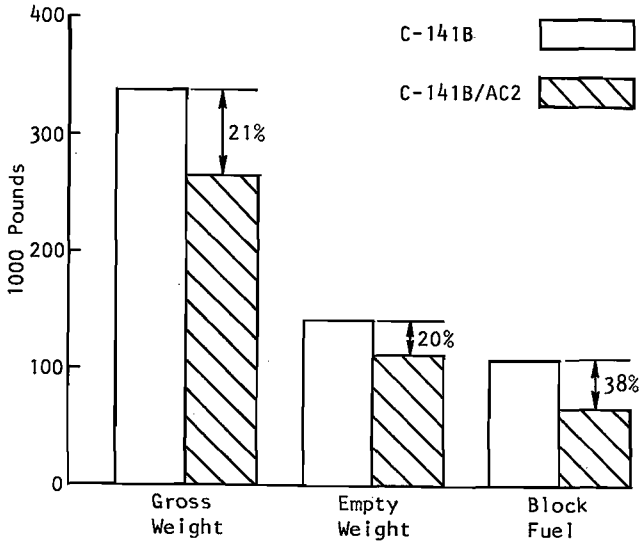

Figure 20. Summary of Aircraft Parameters

Wind tunnel wall pressure data are available for use as far field boundary conditions for each of these configurations.

Correlations between computational results and experimental data have just been started. To date, a viscous version of FL022 developed by Henne has been used to generate solutions for both the designed wing and the measured manufactured wind tunnel model. In the latter case, the wing spanwise twist was adjusted to simulate model deformation under load. The twist distribution was selected to provide the best match between computed and experimental pressures. Uncorrected test data were used in these early comparisons, and free-air far field boundary conditions were used in the calculations.

Isolated wing calculated and measured lift, stability, and drag polar curves are compared in Figures 21, 22, and 23, respectively, for .80 Mach. These comparisons show that the use of measured model ordinates and adjusted twist improve the agreement between calculated and measured wing aerodynamics. The difference between computed and test zero lift angle of attack is in part due to wind tunnel wall effects. The pitching moment discrepancy can be explained by examination of the chordwise pressure distributions.

Computed and measured C-141B/AC2 isolated wing pressures are compared in Figure 24. The use of measured ordinates and adjusted twist improves the correlation. However, the flow near the leading edge and in the lower surface cove region are mispredicted. The discrepancy on the cove pressures is clearly due to flow separation which was not modeled. The differences near the leading edge have not yet been resolved.

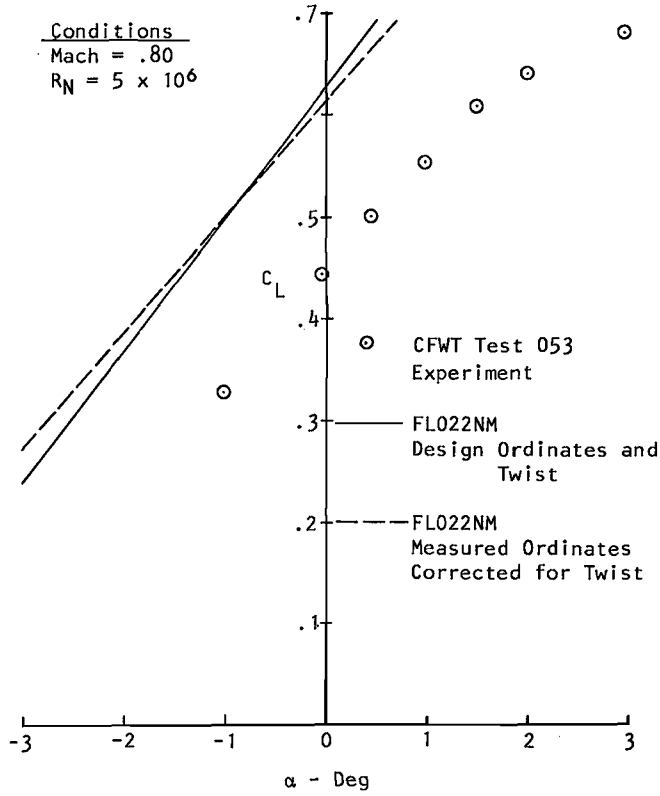

Figure 21. C-141B/AC2 Isolated Wing Measured and Computed Lift

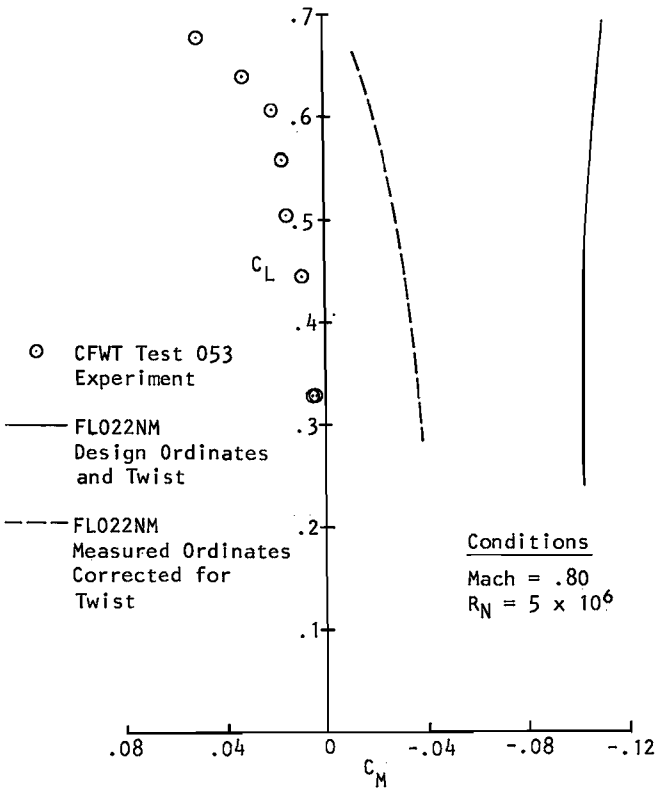

Figure 22. C-141B/AC2 Isolated Wing Measured and Computed Stability

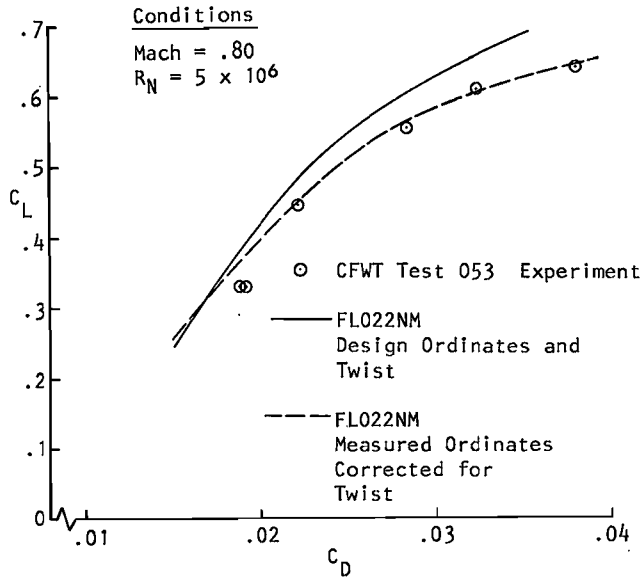

Figure 23. C-141B/AC2 Isolated Wing Measured and Computed Drag Polar

Of particular note in the pressure distributions is the presence of a shock wave with an approximately constant sweep angle. This weak swept shock wave was specified in the target pressures used to design the wing. The shock wave behavior is fairly well predicted when the measured wing geometry with adjusted twist are used in the calculation.

Additional code correlations are now underway. For those correlations, measured model ordinates

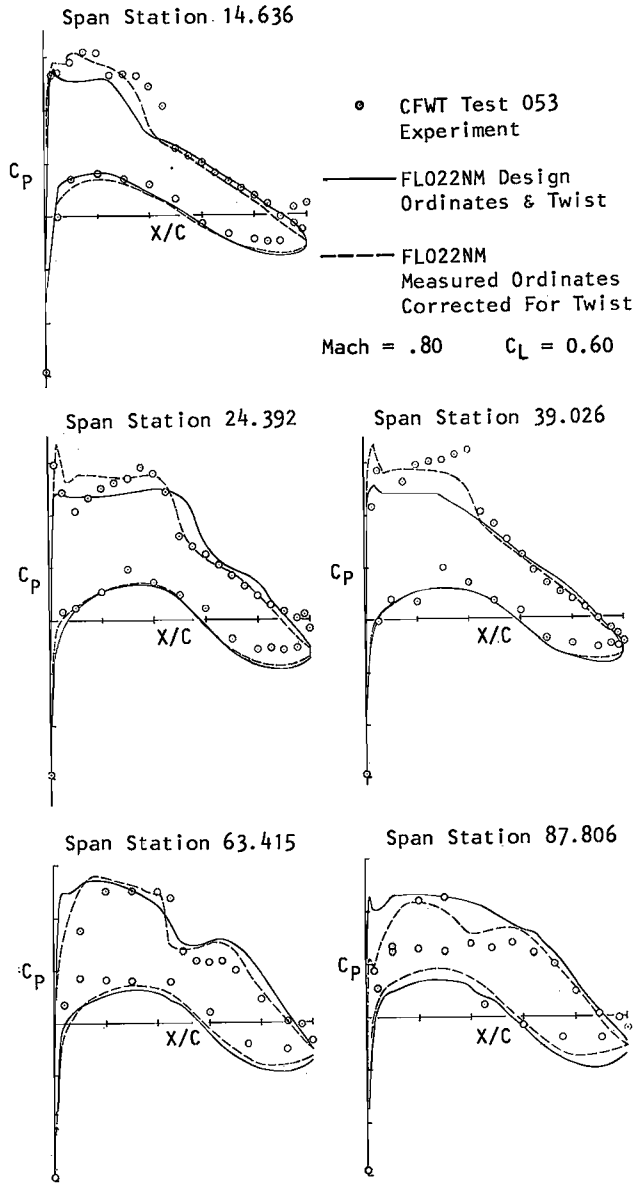

Figure 24. Measured and Computed C-141B/AC2 Isolated Wing Pressures

will be used, and the wing spanwise twist distribution under load will be computed using a procedure similar to that developed in Reference 18. The wind tunnel walls will be taken into account by developing Dirichlet boundary conditions from the measured wall rail pressures [19]. If good correlations result, these analyses of the design wing ordinates and twist with free-air far-field boundary conditions should produce reliable predictions of wing-flight performance.

The ability to accurately analyze complex configurations is clearly needed. The systematic configuration build-up used in this program's wind tunnel test provides a consistent data set for evaluating the accuracy of solutions computed for increasingly complex configurations (e.g., isolated wing, wing-body, wing-body-pylon/nacelle, etc.). Candidate codes for this evaluation are the extended small disturbance codes reported in References 20 and 21, and the full potential equation methods being developed by Jameson and Caughey.

Critique of Design Procedure

This study has shown that numerical optimization provides a means to design wings which produce desired cruise pressure distributions and that the method can be incorporated within the framework of current aircraft design procedures. However, three basic deficiencies have been identified in the current design procedure:

1. Design variable deficiencies
2. Excessive user expertise
3. Excessive computation time

These deficiencies as well as possible correction will now be discussed.

Design Variable Deficiencies

Sine deformation shape functions of the form $\sin^n(\pi x)$ provide the primary means of modifying the wing geometry to produce the desired pressures. The intent of these functions is to provide local geometric control. For example, the shape function $\sin^3 \pi x$ produces maximum geometric change at the 50% chord station as shown in Figure 25. Also shown in that figure is the change in curvature produced by the shape function. Although the maximum curvature change occurs at 50% chord, there are two other locations of significant curvature change. Since curvature plays a dominant role in the development of the flow field, the non-localized curvature changes produced by the sine shape functions can cause undesired changes in the flow field and that introduces ambiguity in the optimization process.

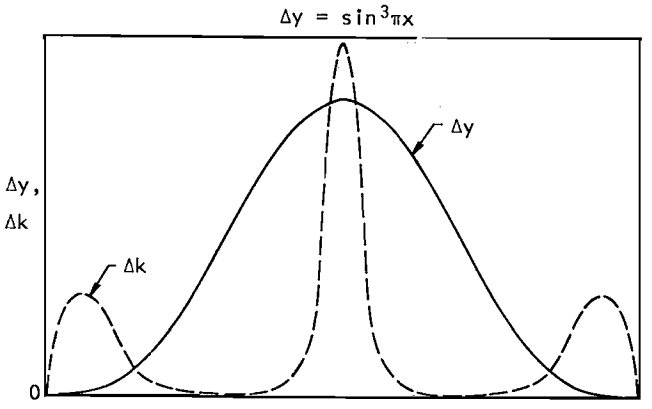

Figure 25. Airfoil Ordinate and Curvature Change

A remedy for this deficiency is to use design variables based on the second derivative of the airfoil surface. Such shape functions not only localize the curvature variations, but also produce very smooth airfoils. Research is presently underway at Lockheed-Georgia and at the Ames Research Center, NASA, to develop efficient curvature-based design variables.

Excessive User Expertise

Engineers who are skilled aerodynamicists and who are familiar with numerical optimization are needed to successfully use optimization in aircraft design. This need exists because of (1) the requirement to accurately specify desirable pressure distributions which produce realistic wing geometries, and (2) difficulties encountered in selecting design shape functions which will produce the desired flow field modifications. The latter difficulty can be ameliorated by the use of curvature-based design variables.

Clearly, the difficulties encountered in the specification of desirable pressure is accentuated for multiple design point aircraft such as supersonic cruise/transonic maneuver fighters. For transport aircraft, consideration of wing weight and drag reduction must be balanced against one another. One possible solution to this problem is the conduct of studies to identify sensible and desirable pressure distributions for different missions. Such a study is being supported by the Office of Naval Research.

Another alternative is the use of design objectives based on aerodynamic forces and moments. For this approach to be successful, the accuracy of computed aerodynamic forces and moments, in particular drag, must be improved. Experience with current numerical aerodynamic methods, even in two dimensions, has shown that inaccuracies in drag calculations can make realistic and reliable numerical optimization difficult. If sufficiently consistent and accurate drag calculation techniques can be developed, then the use of design objectives based on integrated aerodynamic parameters would best take advantage of the capabilities offered by numerical optimization.

Excessive Computation Time

Between 5 to 10 hours of computation time on a CDC 7600-class computer are needed to perform a wing design using the subject numerical optimization scheme. These relatively large times are caused by the multitude of non-linear aerodynamic solutions required during the optimization process. The three obvious ways of reducing the computation times are (1) use more efficient computers, (2) use better solution algorithms, and (3) reduce the number of non-linear solutions.

The first two solutions are related and they involve the use of new algorithms such as approximate factorization schemes on new vector computers such as the CRAY-1 and the CDC Cyber 203. Significant research is being devoted to this task.

The third solution can be approached in at least two ways. One approach is to develop a versatile and reliable 3-D inverse transonic method in which the wing geometry is computed directly from the specified pressures. Such a method would require about the same computation time used in transonic flow analysis. A deficiency in this approach is that constraints are difficult to impose. Nevertheless, an inverse method could produce a wing that is nearly an acceptable design. Numerical optimization could then be used for the final design refinements. The geometric changes might be expected to be less than for a complete optimization design, and fewer design variables might be required. Thus, the number of non-linear solutions needed in the optimization process should be reduced.

The second approach to reducing the number of non-linear solutions in fact involves the replacement of fine grid solutions with coarse grid results.

To maintain accuracy, the coarse grid results are corrected to equivalent fine grid accuracy using Nixon's strained coordinate scheme [22]. The possi- of such an approach is now being investigated by Lockheed-Georgia and Nielsen Engineering and Research Scientists.

Implementation of a design procedure incorporating an inverse method with numerical optimization wing strained coordinates can be expected to reduce wing design computation time from the current 5 to 10 hour range to approximately 1½ to 3 hours on a CDC 7600. By using an algorithm which takes advantage of new vector processing computers, computer-aided wing transonic aerodynamic design in less than ½ hour can be forecast.

Concluding Comments

This study has shown that new computational methods offer a means for the aerodynamic design of wings with transonic performance superior to that which could be obtained using previous design techniques. The method is relatively easy to use, and it is compatible with established industry design procedures. By using the new method, up to a 50% reduction in the cost associated with wing cruise aerodynamic design is obtainable. Planned design method improvements together with the anticipated widespread availability of vector processing computers should make possible efficient wing design using less than ½ hour computation time.

References

1. Blackwell, J. A.: "An Empirical Correction for Wind Tunnel Wall Blockage in Two-Dimensional Transonic Flow." AIAA Paper No. 78-806, April 1978.
2. Blackwell, J. A.: "Scale Effects on Supercritical Airfoils." 11th Congress of the ICAS, Lisbon, Portugal, Sept. 10-16, 1978.
3. Ballhaus, W. F., Bailey, F. R., and Frick, J.: "Improved Computational Treatment of Transonic Flow About Swept Wings." NASA CP-2001, Nov. 1976.
4. Jameson, A.: "Iterative Solution of Transonic Flows Over Airfoils and Wings." Comm. Pure Appl. Math., Vol. 27, 1974, pp. 283-309.
5. Boppe, C. W.: "Computational Transonic Flow About Realistic Aircraft Configurations." AIAA Paper 78-104, Jan. 1978.
6. Mason, W. H., et al.: "An Automated Procedure for Computing the Three-Dimensional Transonic Flow Over Wing-Body Combinations, Including Viscous Effects." AFFDL-TR-77, Oct. 1977.
7. Hicks, R. M., and Henne, P. A.: "Wing Design by Numerical Optimization." AIAA Paper No. 77-1247, Aug. 1977.
8. Haney, H. P., Waggoner, E. G., and Ballhaus, W. F.: "Computational Transonic Wing Optimization Model." AIAA Paper No. 78-102, Jan. 1978.
9. Lores, M. E., Smith, P. R., and Hicks, R. M.: "Supercritical Wing Design Using Numerical Optimization and Comparisons with Experiment." AIAA Paper No. 79-0065, Jan. 1979.
10. Vanderplaats, G. N.: COMMIN-A Fortran Program Constrained Function Minimization-User's Manual. NASA TM X-62282, Aug. 1973.
11. McNally, W. D.: "FORTRAN Program for Calculating Compressible Laminar and Turbulent Boundary Layers in Arbitrary Pressure Gradients," NASA TN D-5681, May 1970.
12. Bartlett, D. W., "Wind Tunnel Investigation of Several High Aspect Ratio Supercritical Wing Configurations on a Wide-Body-Type Fuselage," NASA TM X-71996, 1977.
13. Kline, J., "Wind Tunnel Tests of a 0.030 Scale Full-Span Model of the Lockheed-Georgia ATA Series S Transport," Calspan Rept. AA-4007-W-7, 1978.
14. Carlson, L. A.: "Transonic Airfoil Design Using Cartesian Coordinates," NASA CR-2578, Dec. 1975.
15. Hess, J. L.: "Calculation of Potential Flow About Arbitrary Three-Dimensional Lifting Bodies," McDonnell-Douglas Rept. No. MDC 15679-01, Oct. 1972.
16. Pounds, G. A., and Stanewsky, E.: "The Research Compressible Flow Facility, Part 1 - Design," Lockheed-Georgia Company ER-9219-1, 1967.
17. Pounds, G. A., and Walker, J.: "Semispan Model Testing in a Variable Porosity Wind Tunnel," AIAA Paper No. 80-0461, March 1980.
18. Chipman, R., Walter, C., and MacKenzie, D.: "Numerical Computation of Aeroelastically Corrected Transonic Loads," AIAA Paper No. 79-0766, April 1979.
19. Hinson, B. L., and Burdges, K. P.: "An Evaluation of Three-Dimensional Transonic Codes Using New Correlation-Tailored Test Data," AIAA Paper No. 80-0003, January 1980.
20. Boppe, C. W., and Stern, M. A.: "Simulated Transonic Flows for Aircraft With Nacelles, Pylons, and Winglets," AIAA Paper No. 80-0130, Jan. 1980.
21. Srokowski, A. J., Shrewsbury, G. D., and Lores, M. E.: "A Transonic Mutual Interference Program for Computing the Flow About Wing-Pylon/Nacelle Combinations," to be published as AIAA Paper No. 80-1333, June 1980.
22. Nixon, D.: "Perturbation of a Discontinuous Transonic Flow," AIAA Paper No. 77-206, 1977.